Analysis of texture features of CT-images in abdomen organs segmentation

Alexandra Yurova, MSU, MIPT

November 2, 2016

Outline

- Segmentation: definition and applications

Outline

- Segmentation: definition and applications
- Input data and problems

Outline

- Segmentation: definition and applications
- Input data and problems
- Our approaches to abdominal cavity segmentation

Outline

- Segmentation: definition and applications
- Input data and problems
- Our approaches to abdominal cavity segmentation
- Results

Outline

- Segmentation: definition and applications
- Input data and problems
- Our approaches to abdominal cavity segmentation
- Results
- References

Segmentation in ITK-SNAP

www.itksnap.org

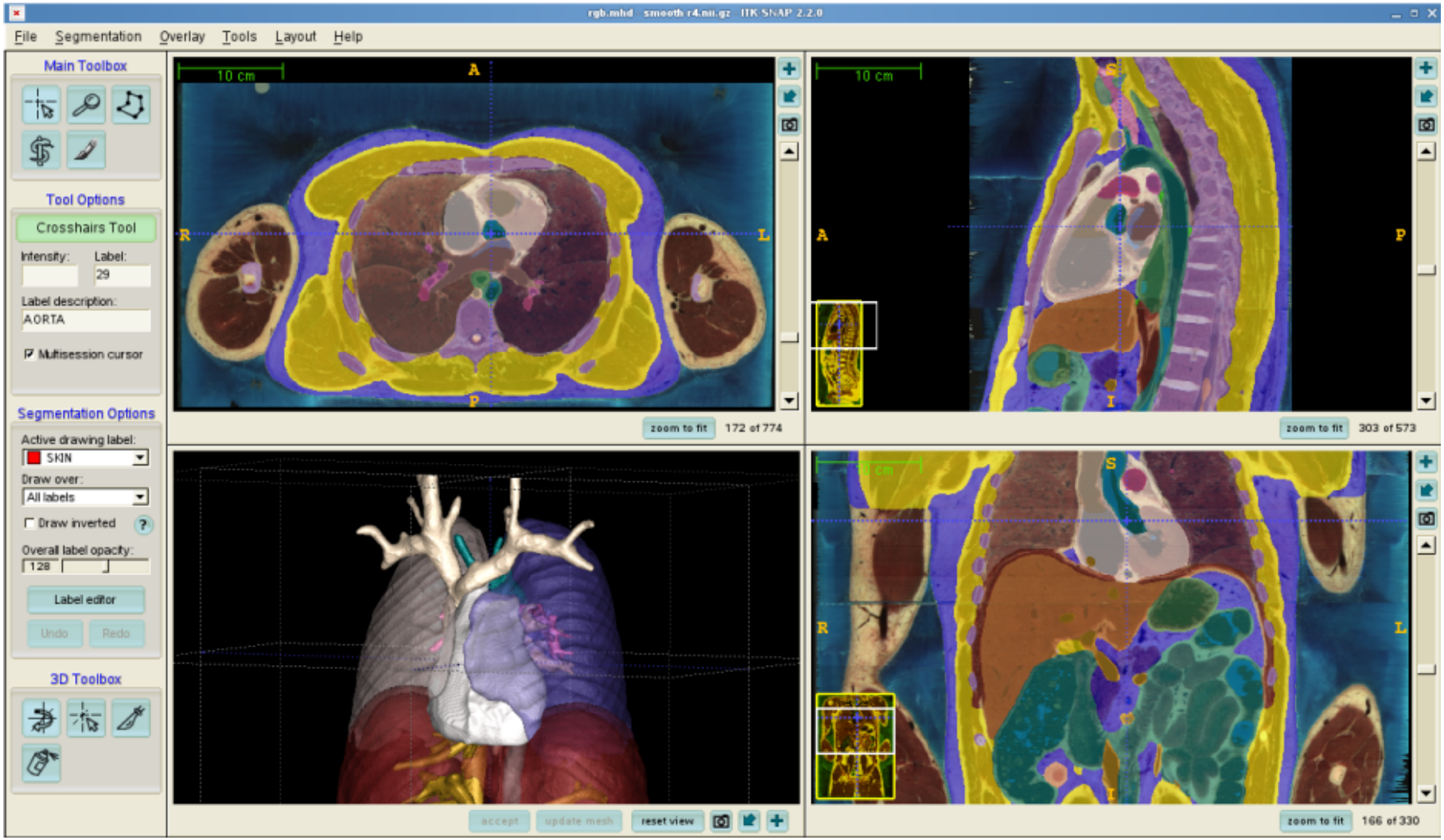

Medical image segmentation

Fullsize segmented model and tetrahedral mesh

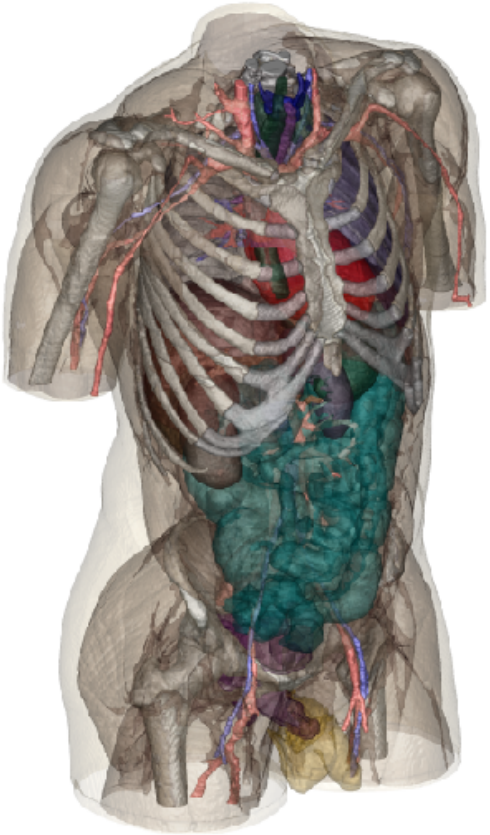

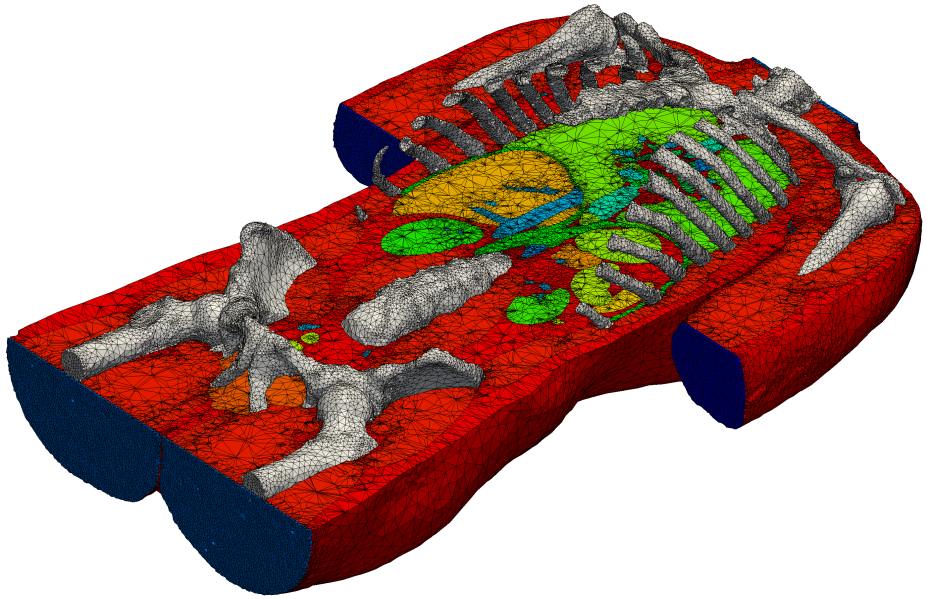

Input data: Examples of CT scans

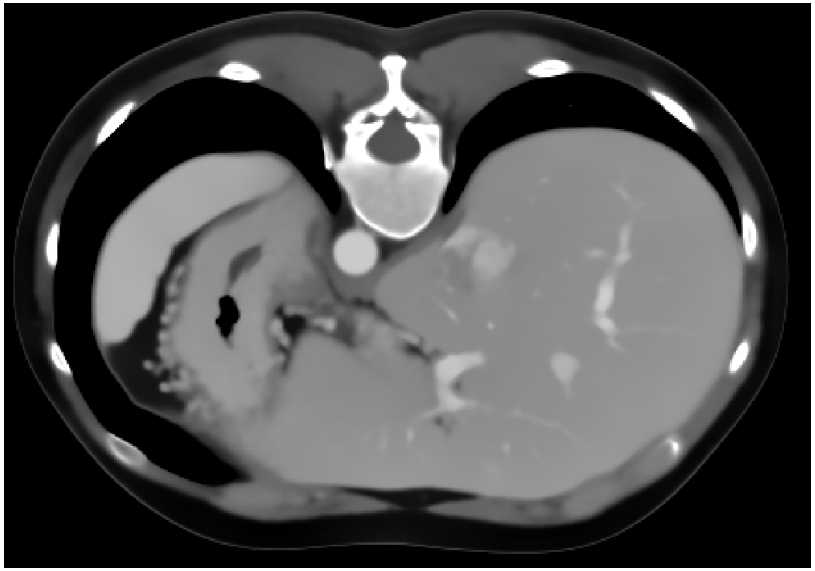

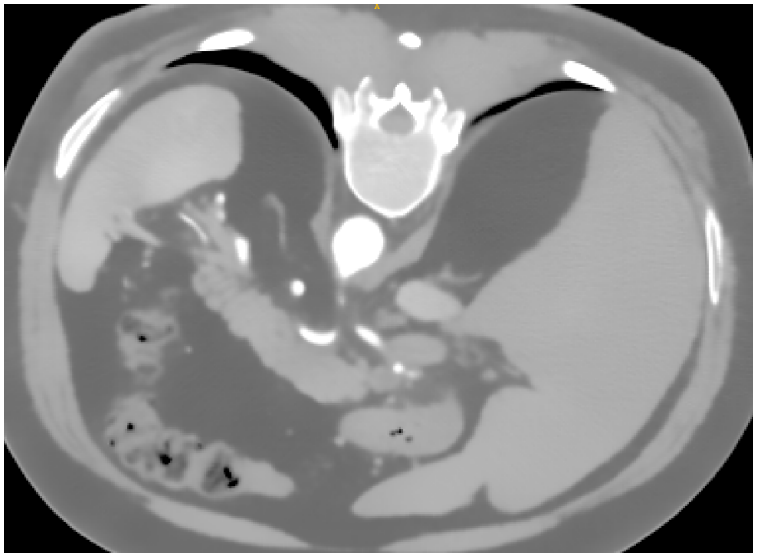

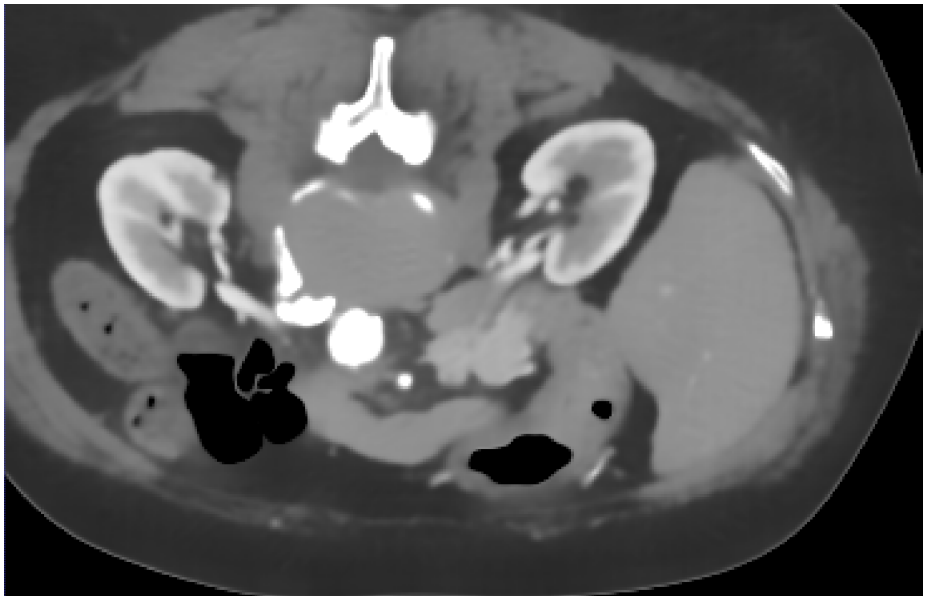

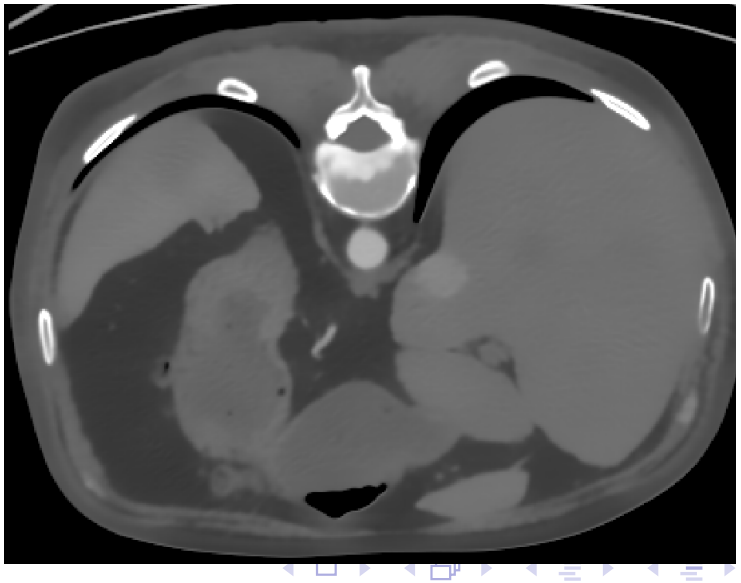

Main problems

- image variability resulting from the wide range of imaging devices

Main problems

- image variability resulting from the wide range of imaging devices
- noise, artifacts

Main problems

- image variability resulting from the wide range of imaging devices
- noise, artifacts
- large patient anatomical variability

Main problems

- image variability resulting from the wide range of imaging devices
- noise, artifacts
- large patient anatomical variability
- intensity values overlap between different organs("leaks")

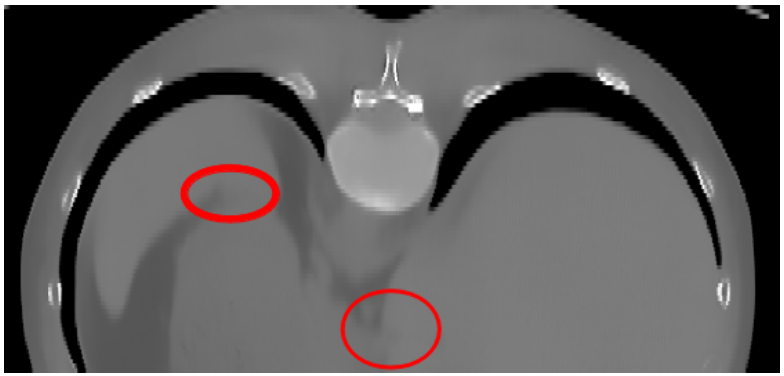

Main problems

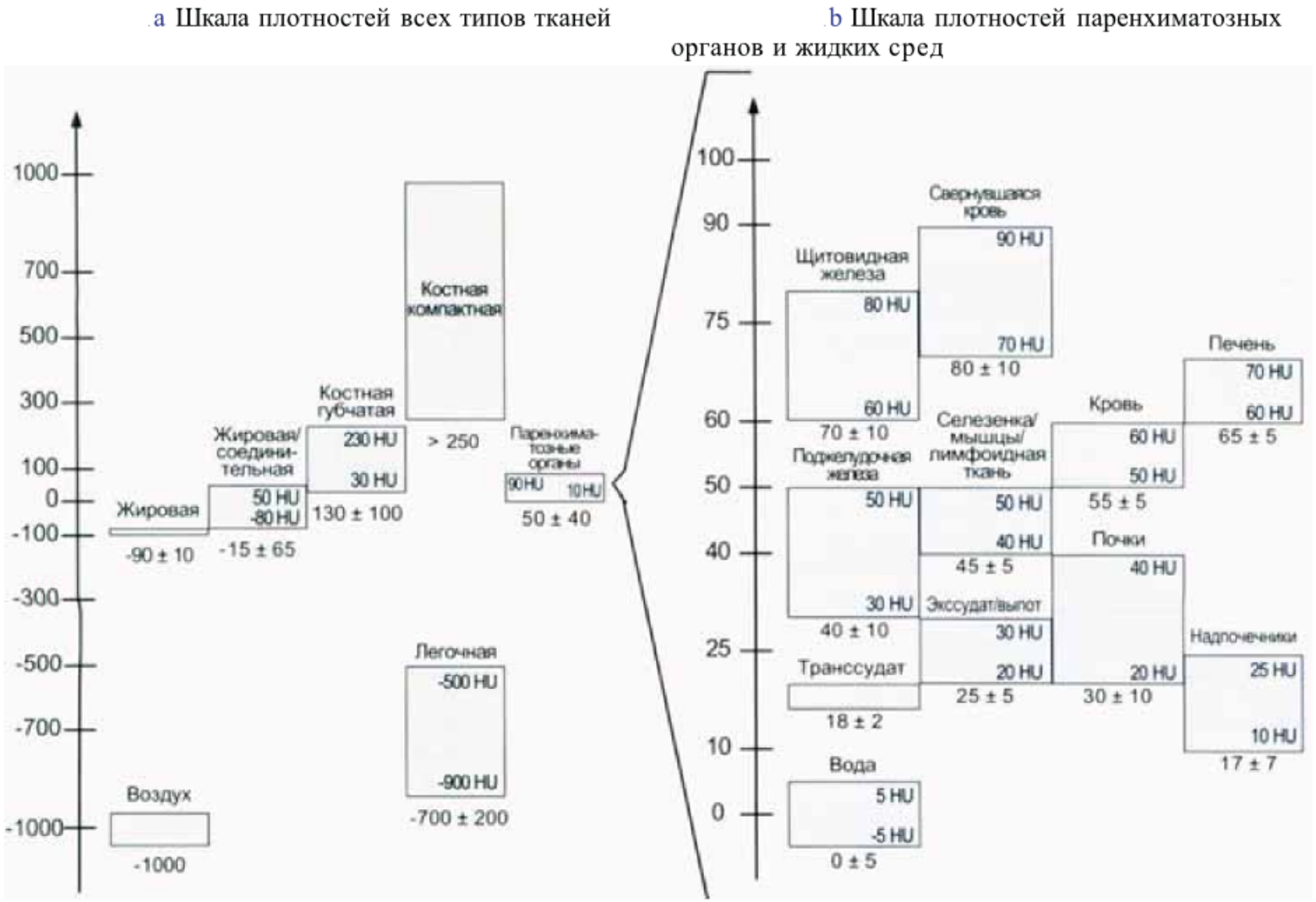

Matthias Hofer. “CT-Kursbuch“. Didamed Verlag, 2014

Main problems: partial volume effect

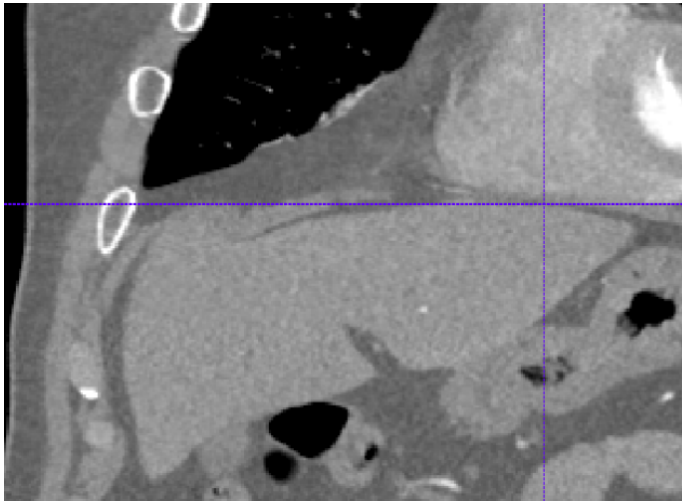

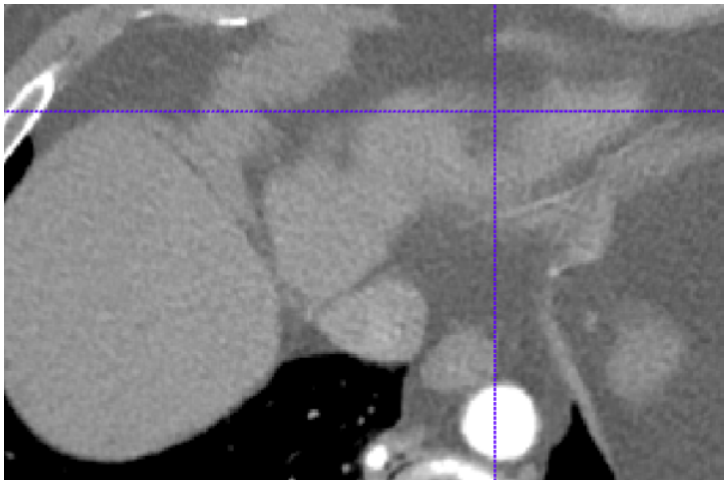

Coronal and axial slices of liver

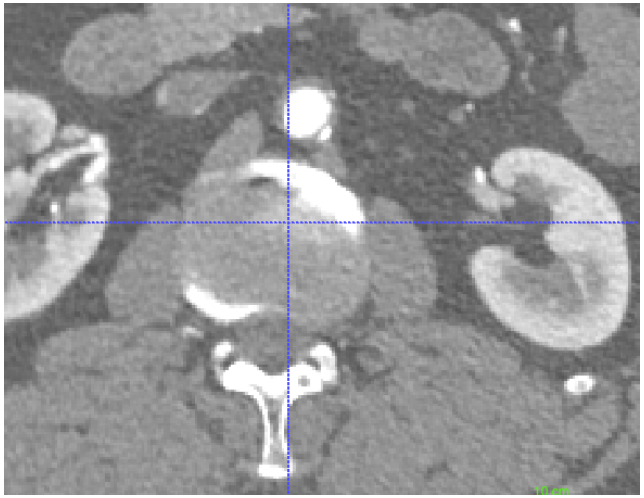

Coronal and axial slices of spine

Previous work: reference model transformation

- Anthropometrical rescaling of the human model

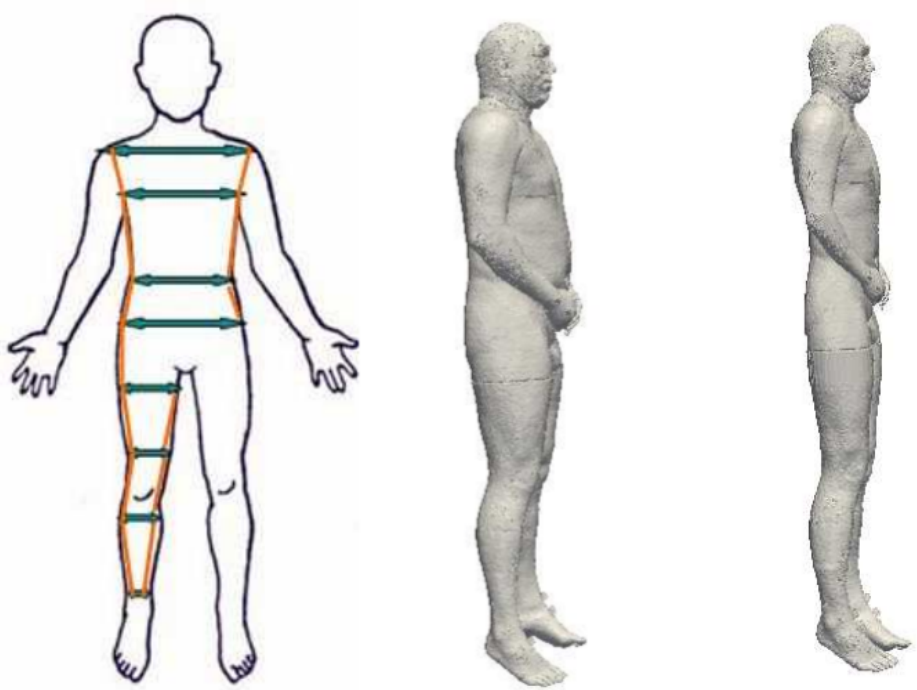

Danilov, A.; Kramarenko, V.; Nikolaev, D.; Yurova, A. Personalized model adaptation for bioimpedance measurements optimization. Russian Journal of Numerical Analysis and Mathematical Modelling 2013, 28, 459–470.

Previous work: reference model transformation

- two sets of the control points defined by user
- the control points of the reference image are shifted to the new positions

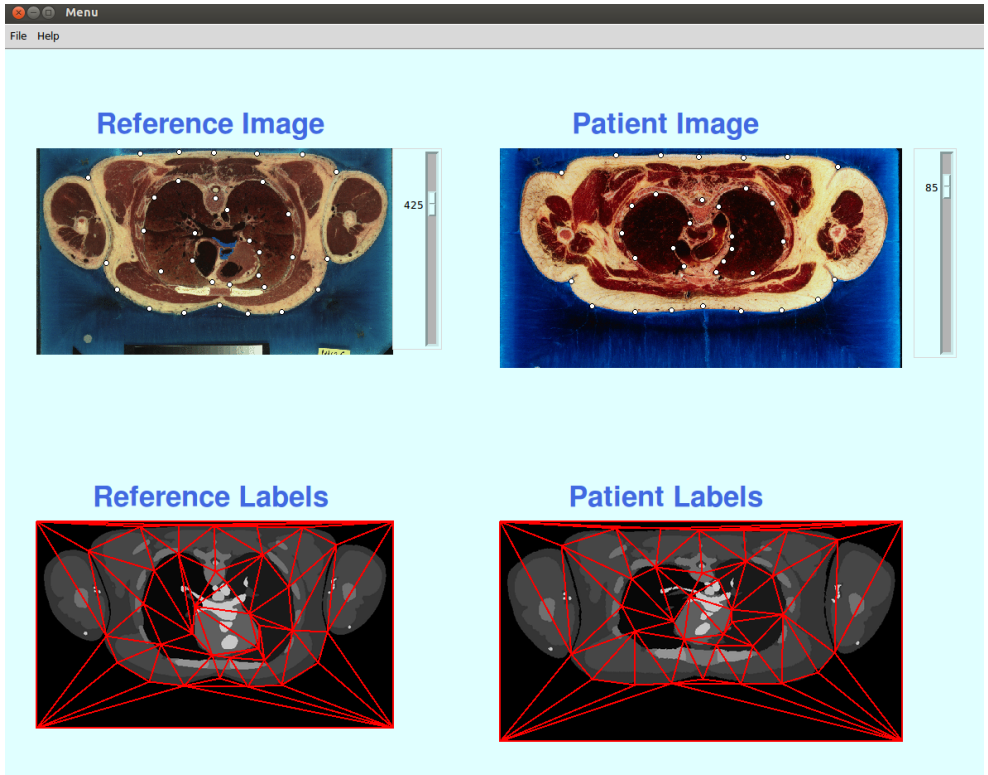

Danilov, A.; Kramarenko, V.; Nikolaev, D.; Yurova, A. Personalized model adaptation for bioimpedance measurements optimization. Russian Journal of Numerical Analysis and Mathematical Modelling 2013, 28, 459–470.

Previous work: voxel clustering

- Simple Linear Iterative Clustering (SLIC) and Region Adjacency Graph. Edge weights depend on the clusters mean intensity.

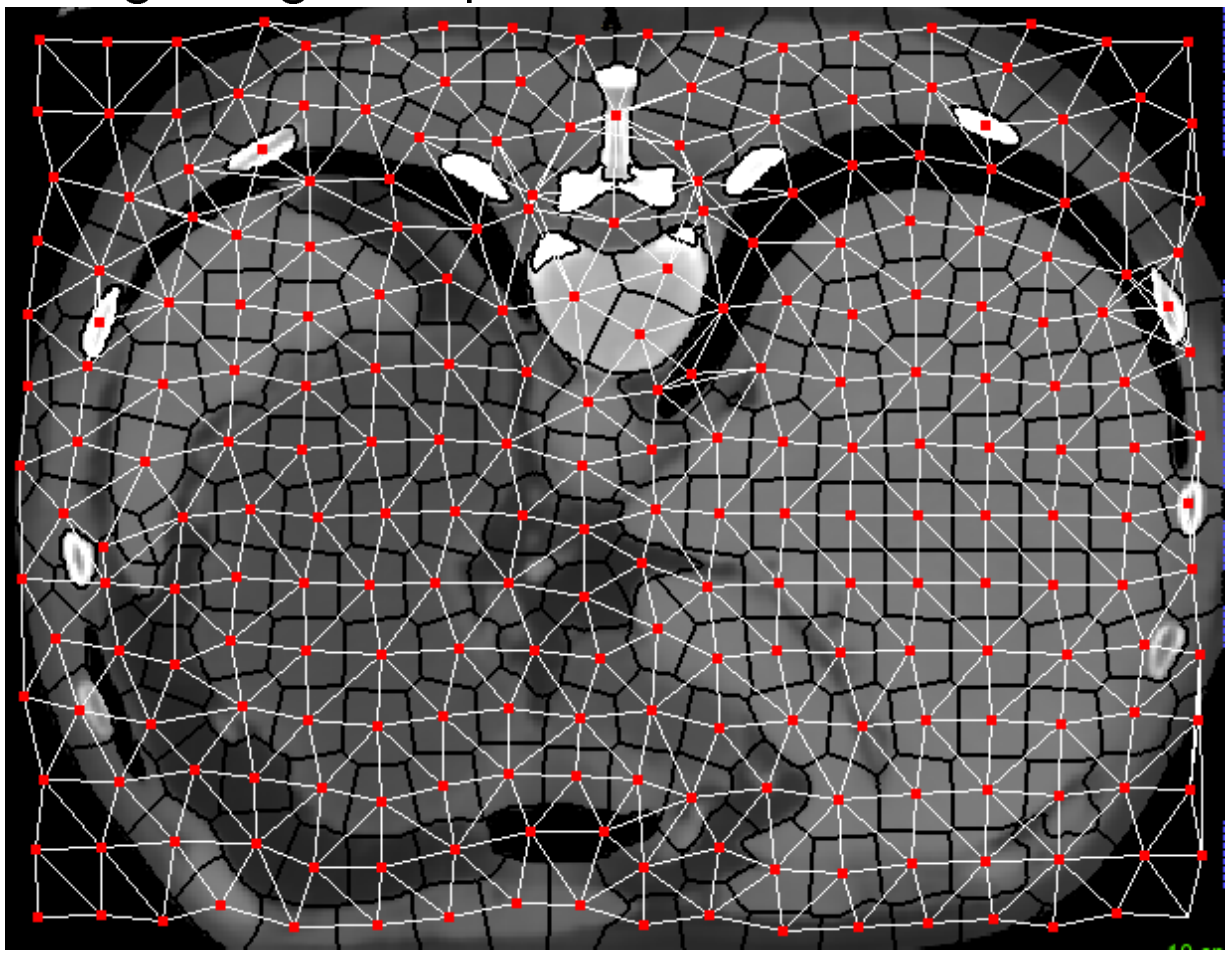

Previous work: voxel clustering

- Egdes are removed by thresholding

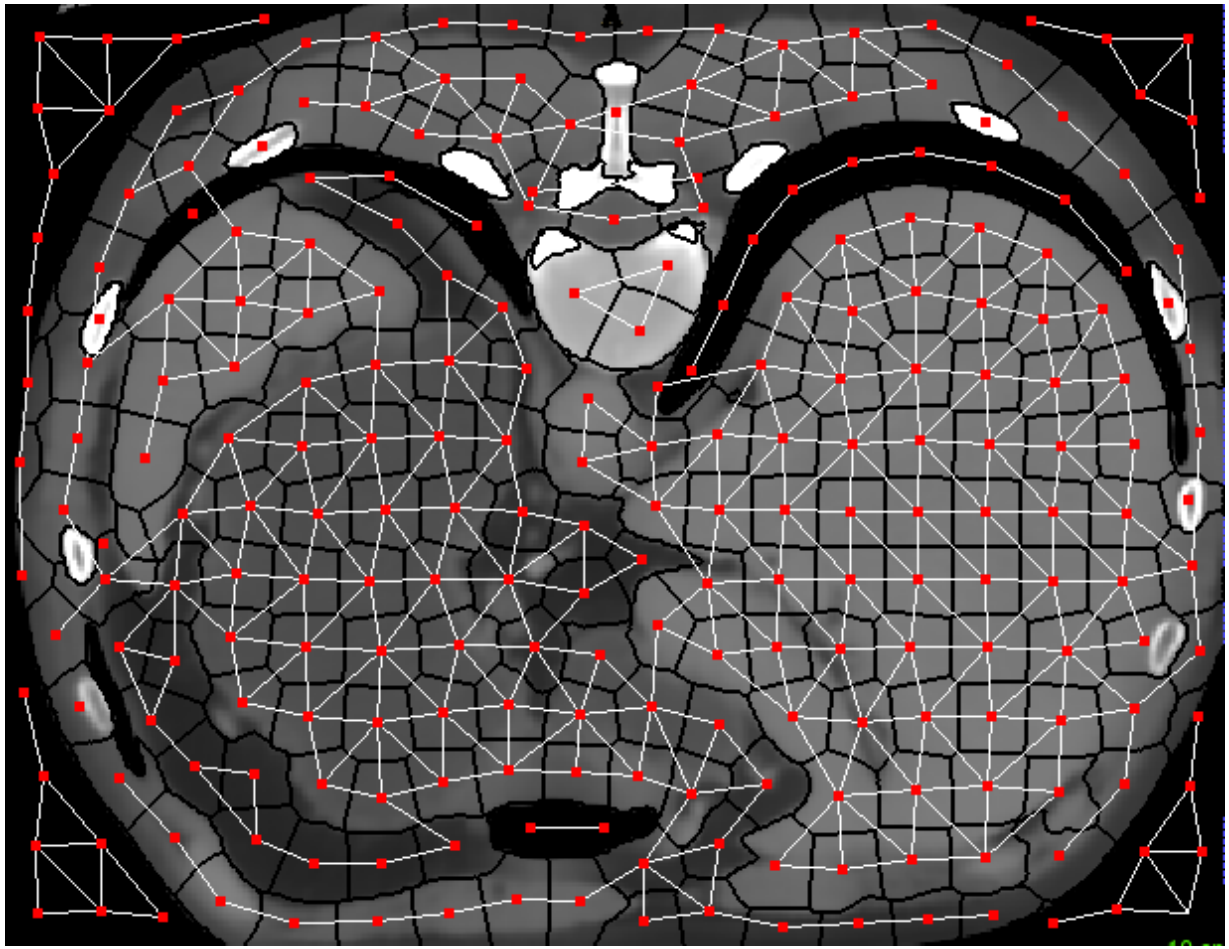

Previous work: voxel clustering

- Egdes are removed by thresholding

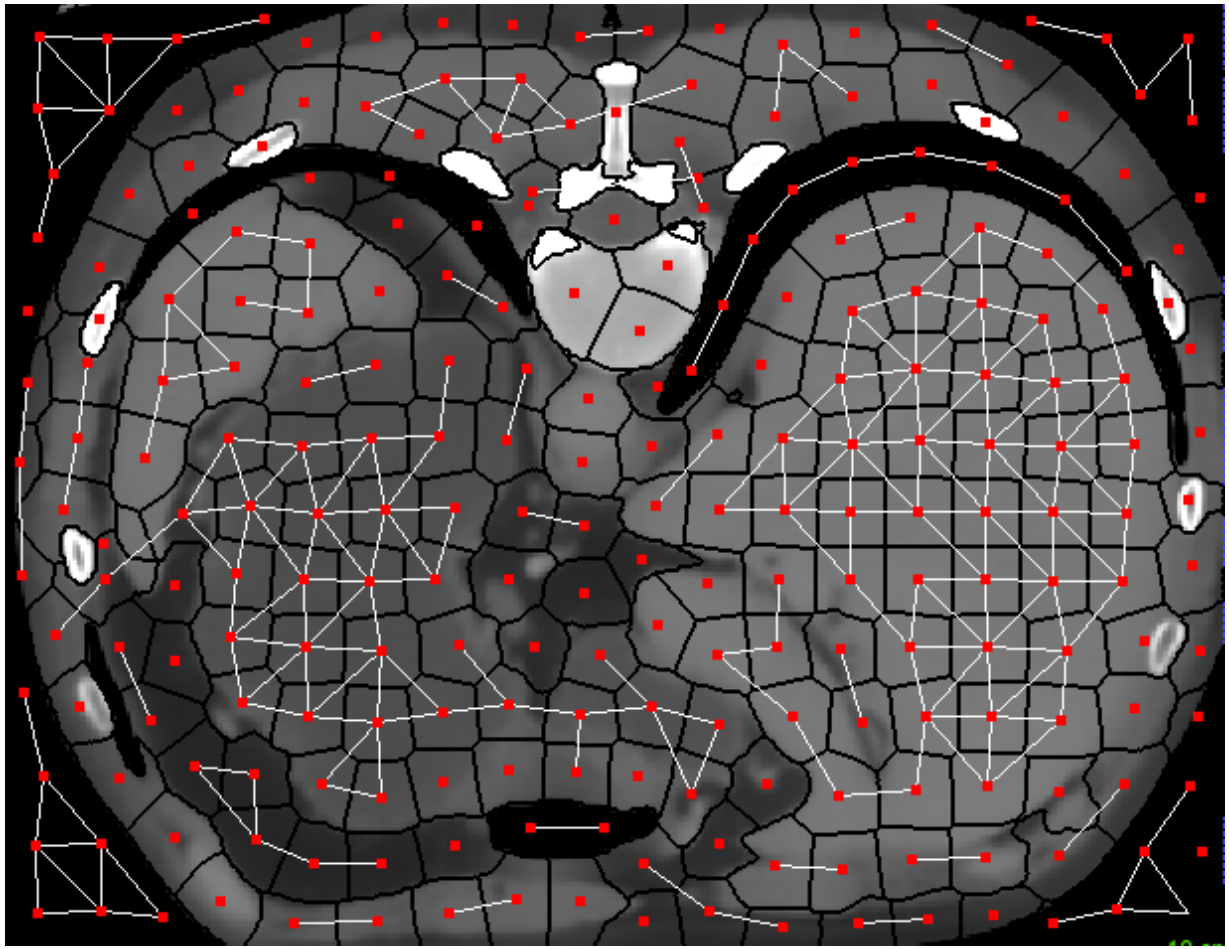

Previous work: edge detectors

Additional information: Edge detectors(Canny edge detector)

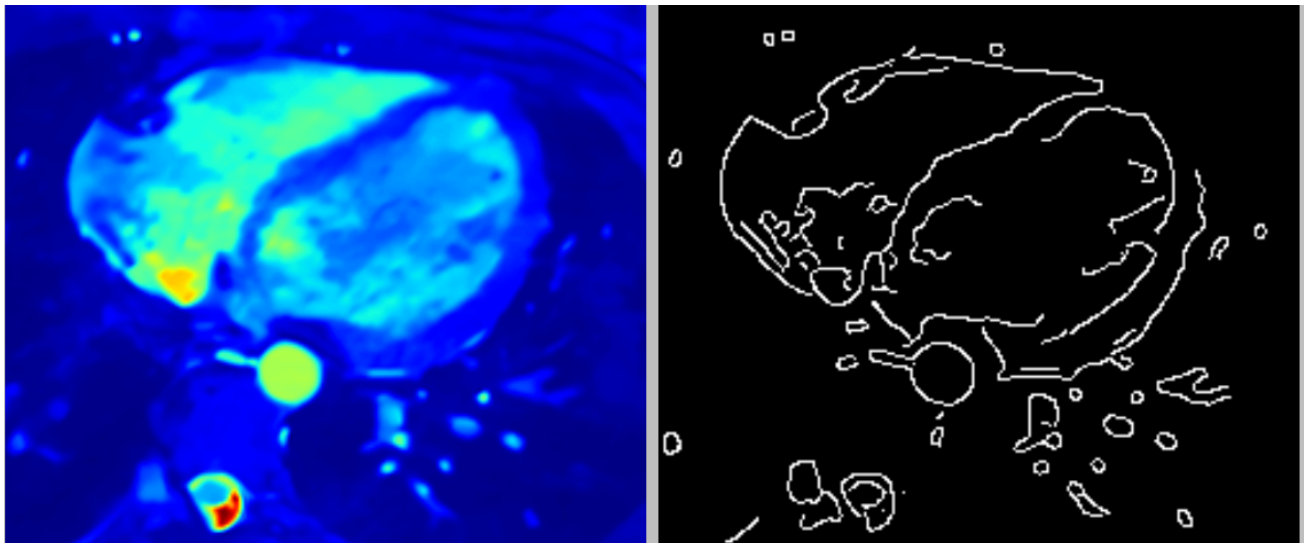

Drawbacks:

- false edges
- discontinuities

Previous work: edge detectors

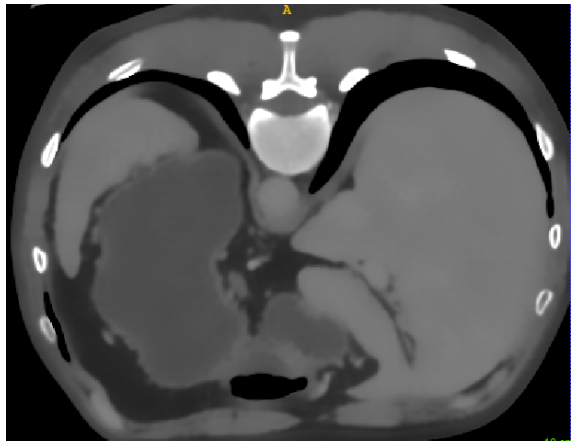

Abdominal cavity CT

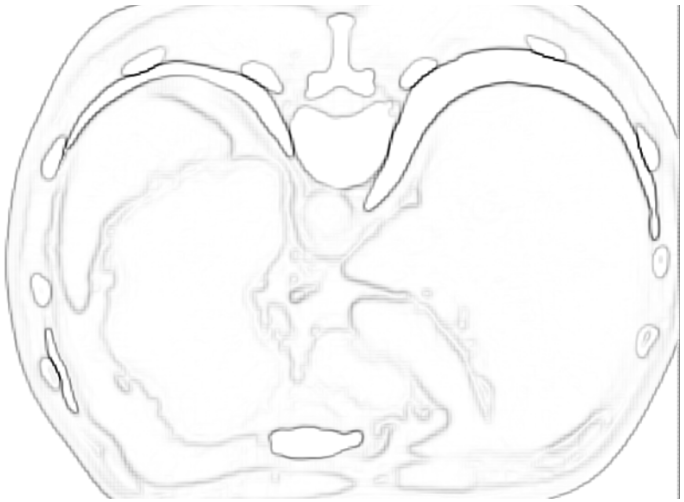

Prewitt operator

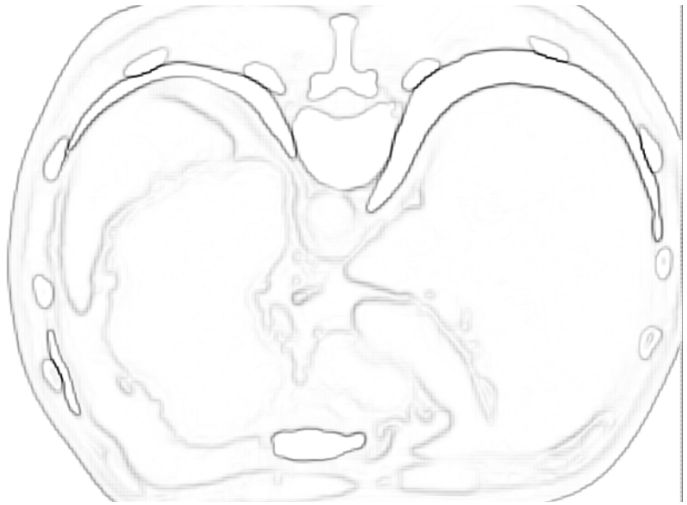

Sobel operator

Texture analysis for medical image segmentation

R.Haralick, K.Shanmugam. Textural Features for Image Classification.

1. texture contains important information about the structural arrangement of surfaces and their relationship to the surrounding environment
2. for human observers texture is quite easy to recognize and describe in empirical terms

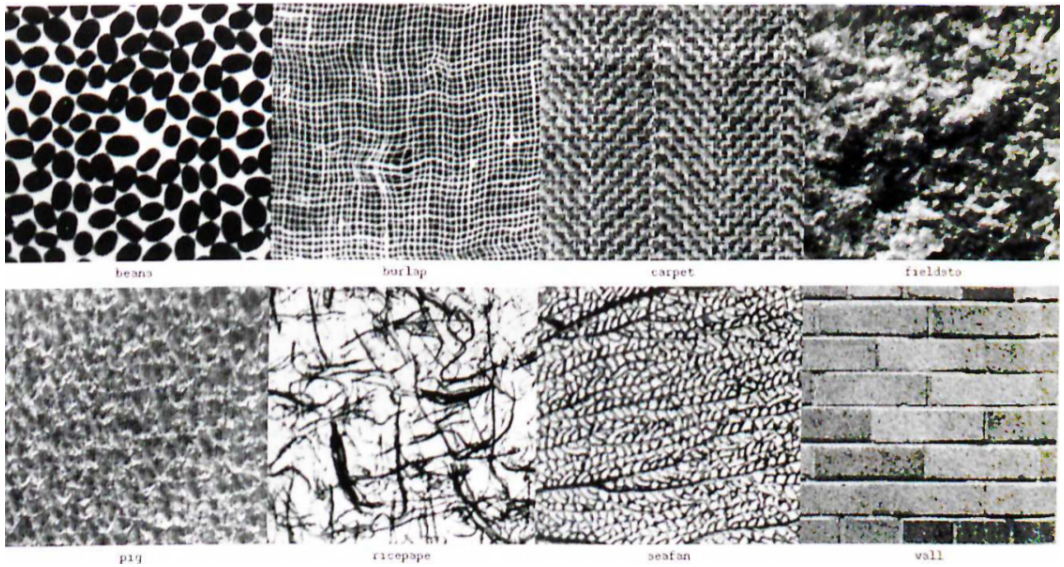

Texture analysis for medical image segmentation

R.Haralick, K.Shanmugam. Textural Features for Image Classification.

- Image $N_x \times N_y$
- $L_x = \{1, 2, ..., N_x\}$, $L_y = \{1, 2, ..., N_y\}$
- The set of quantized gray tones: $G = \{1, 2, ..., N_g\}$

Gray-Tone Spatial-Dependence Matrices:
a frequency of occurance of two neighboring resolution cells separated by distance d, with gray tones i and j.
I.e. for any horizontal distance d in 2D case the matrix is computed as following:

$$P(i, j, d, 0) = \#\{((k, l), (m, n)) \in (L_x \times L_y) \times (L_x \times L_y)) | k - m = 0, |l - n| = d, I(k, l) = i, I(m, n) = j\},$$

where $\#$ denotes the number of elements in the set.

Texture analysis for medical image segmentation

Examples of Textural Features Extracted from Gray-Tone Spatial-Dependence Matrices

- Angular second moment
  $f_1 = \sum_i \sum_j \{p(i,j)\}^2$
- Contrast
  $f_2 = \sum_{n=0}^{N_g-1} n^2 \{ \sum_{\substack{i=1 \\ |i-j|=n}}^{N_g} \sum_{j=1}^{N_g} p(i,j) \}$
- Inverse Difference Moment
  $f_3 = \sum_i \sum_j \frac{1}{1+(i-j)^2} p(i,j)$
- Entropy
  $f_4 = -\sum_i \sum_j p(i,j) \log(p(i,j))$

Texture analysis for medical image segmentation

Rules of automated segmentation:

- Garbage In = Garbage Out

Texture analysis for medical image segmentation

Rules of automated segmentation:

- Garbage In = Garbage Out
- Automatic segmentation is weaker than manual segmentation, but it saves time

Texture analysis for medical image segmentation

Multiphase CT-scans

a. Native phase b. Arterial phase c. Venous phase

H. Alkadhi, S. Leschka, P. Stolzmann, H. Scheffel. "Wie funktioniert CT?". Springer, 2011

Texture analysis for medical image segmentation

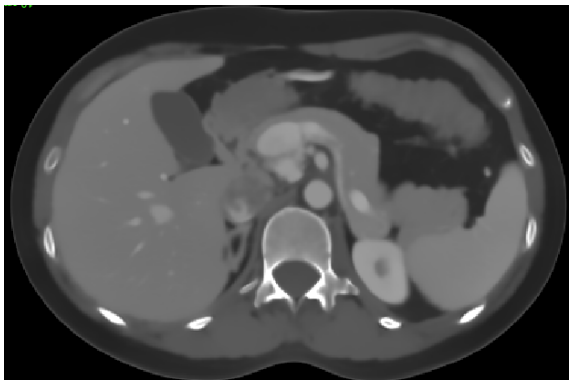

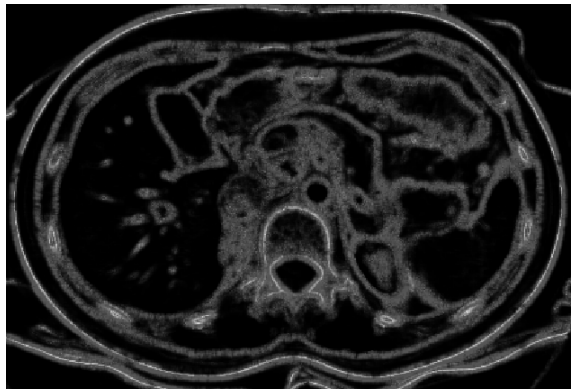

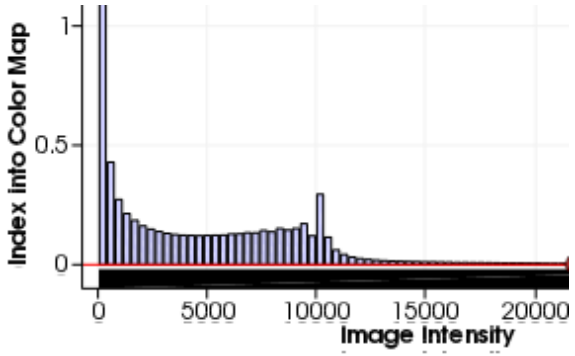

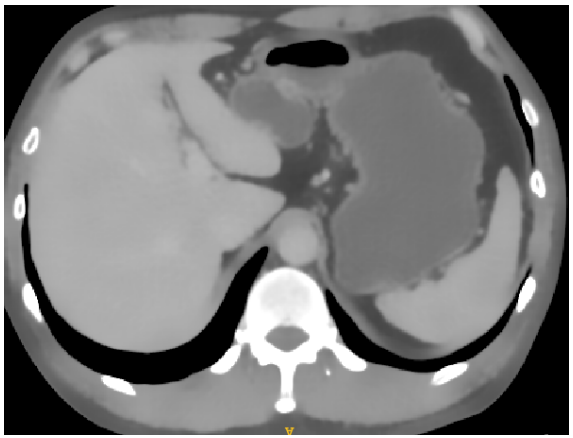

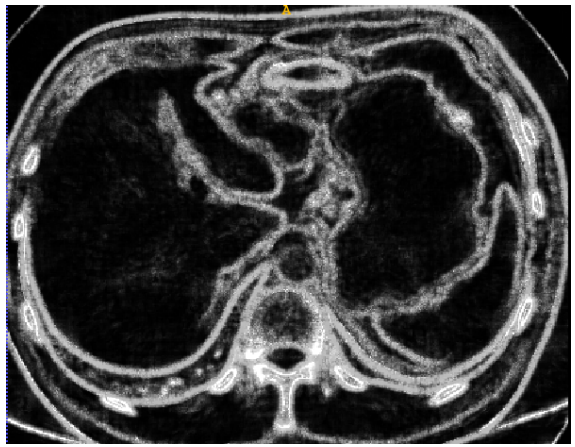

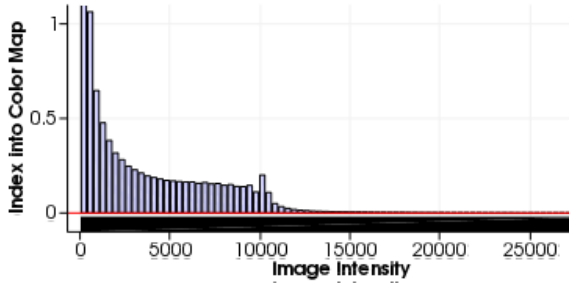

Results of contrast computation for two anonymous patients

Texture analysis for medical image segmentation

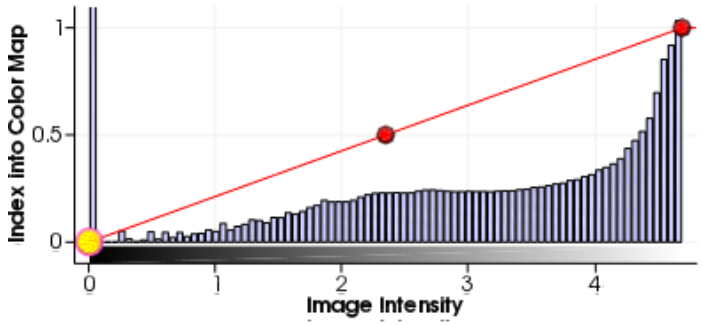

$3 \times 3 \times 3$ vox neighborhood

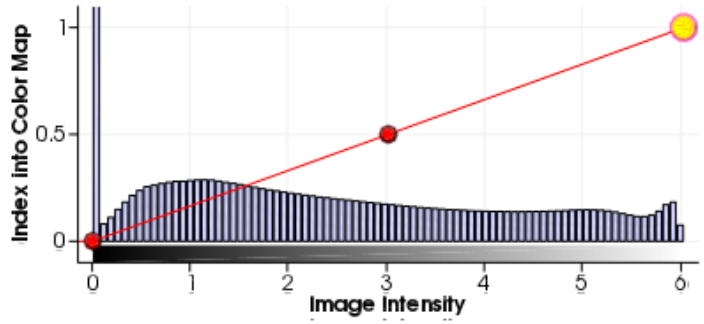

$5 \times 5 \times 5$ vox neighborhood

Results of entropy computation for anonymous patient on two different scales

$$ENT_{\mathbf{d}} = -\sum_{i=0}^{g}\sum_{j=0}^{g} p_{\mathbf{d}}(i,j)\ln(p_{\mathbf{d}}(i,j))$$

- Entropy achieves its maximum value $\ln r$, if the number of different adjacent voxel pairs is equal to the number of connections in the neighborhood
  r is the doubled number of connections in the cubic neighborhood.
- Entropy achieves its minimum value, if there is only one type of connection.

Texture analysis for medical image segmentation

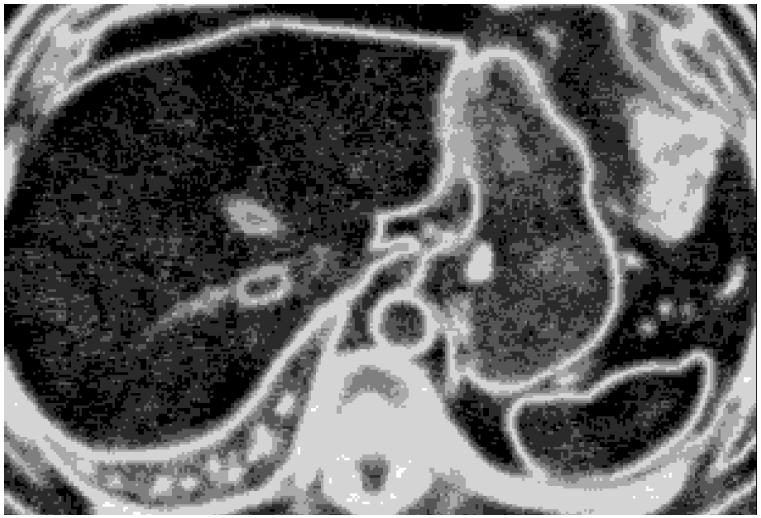

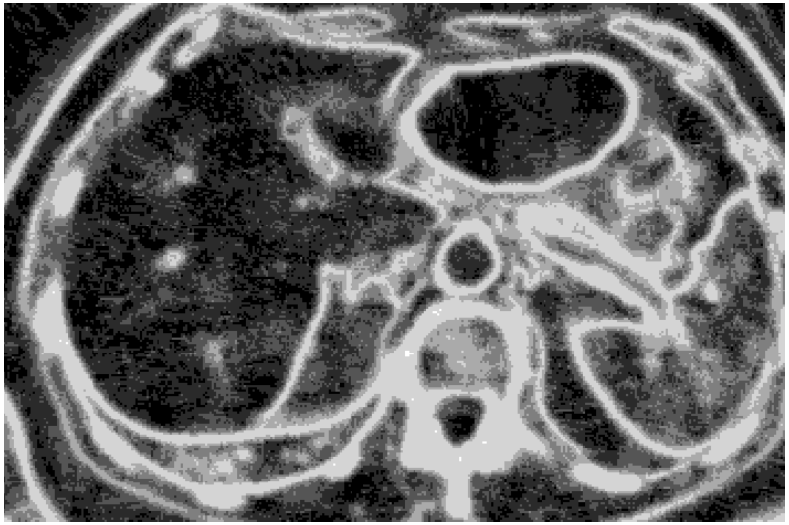

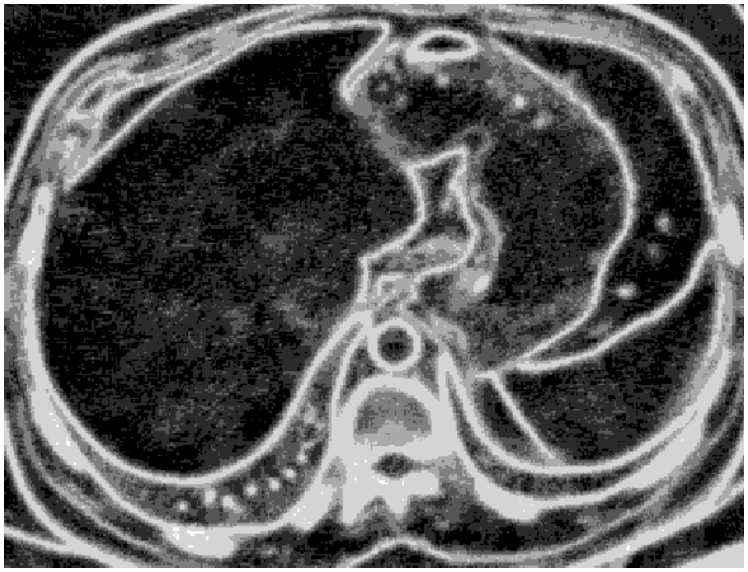

Texture analysis for medical image segmentation

Binary mask obtained from the results of entropy computation

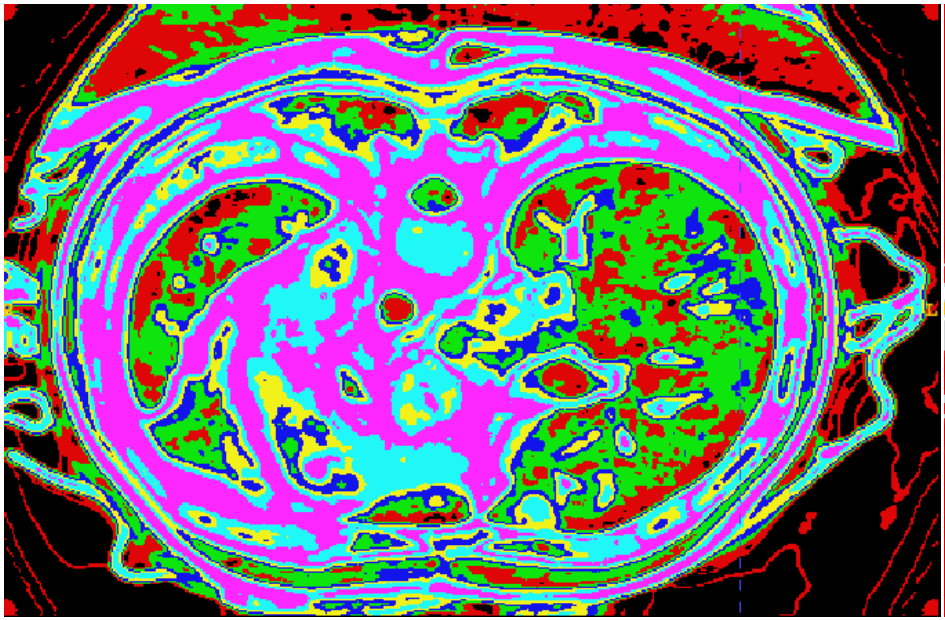

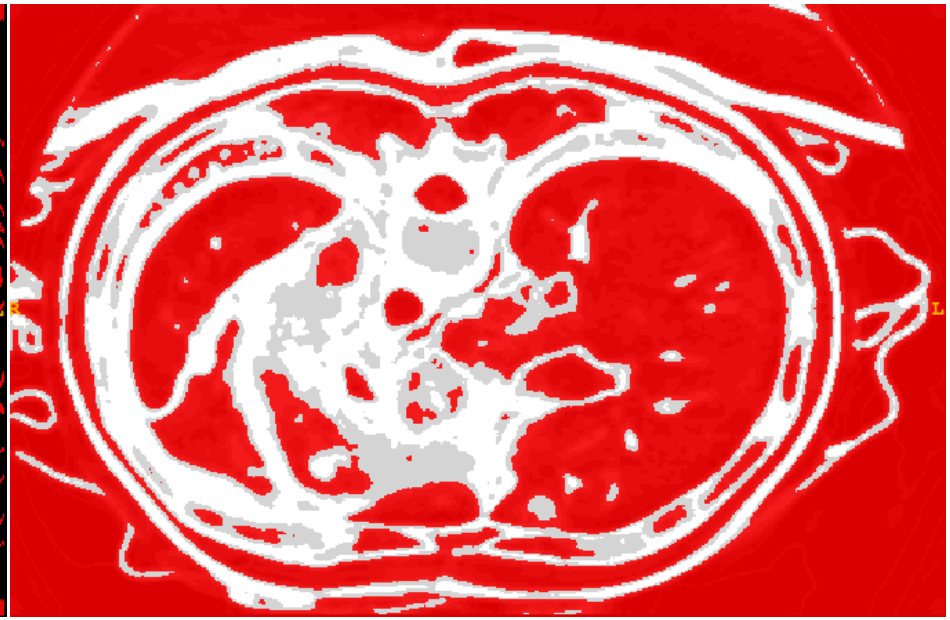

Extraction of 3D model: 3D active contours

Active contour evolution is driven by a combination of forces:

1. **External forces (image-driven)**
   push the contour towards boundaries in the image data
2. **Internal forces (shape-driven)**
   push the contour towards maintaining a simple shape

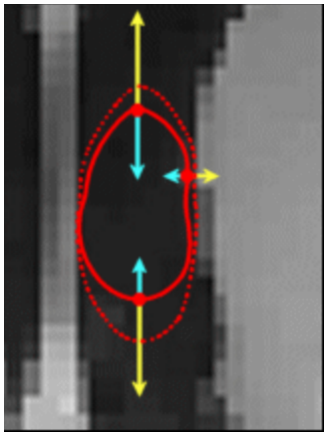

(picture from ITK SNAP guide)

Yushkevich P.A., Piven J., Hazlett H.C., Smith R.G., Ho S., Gee J.C., Gerig G. User-guided 3D active contour segmentation of anatomical structures: significantly improved efficiency and reliability

Results

Spleen segmentation

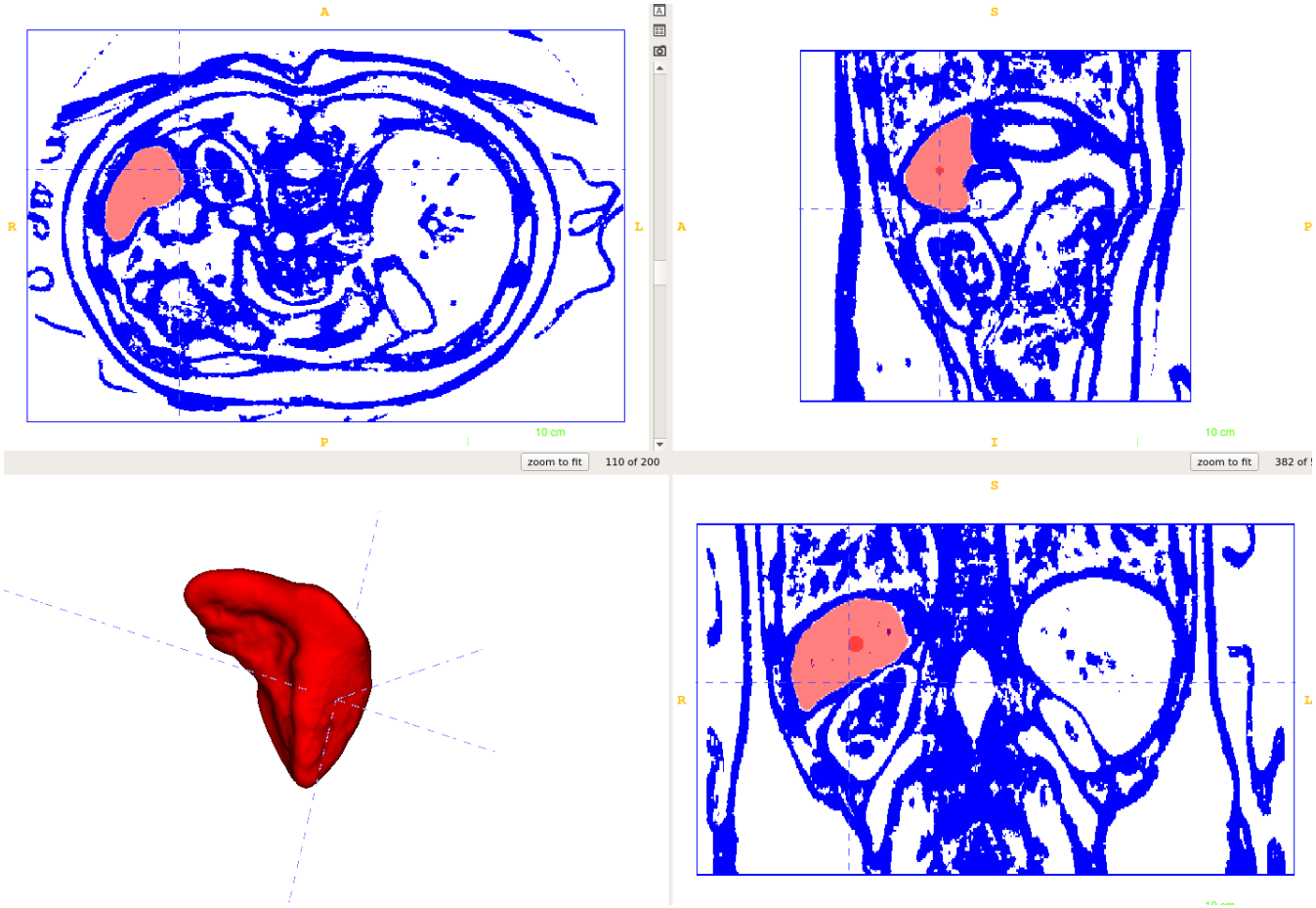

Results

Liver segmentation

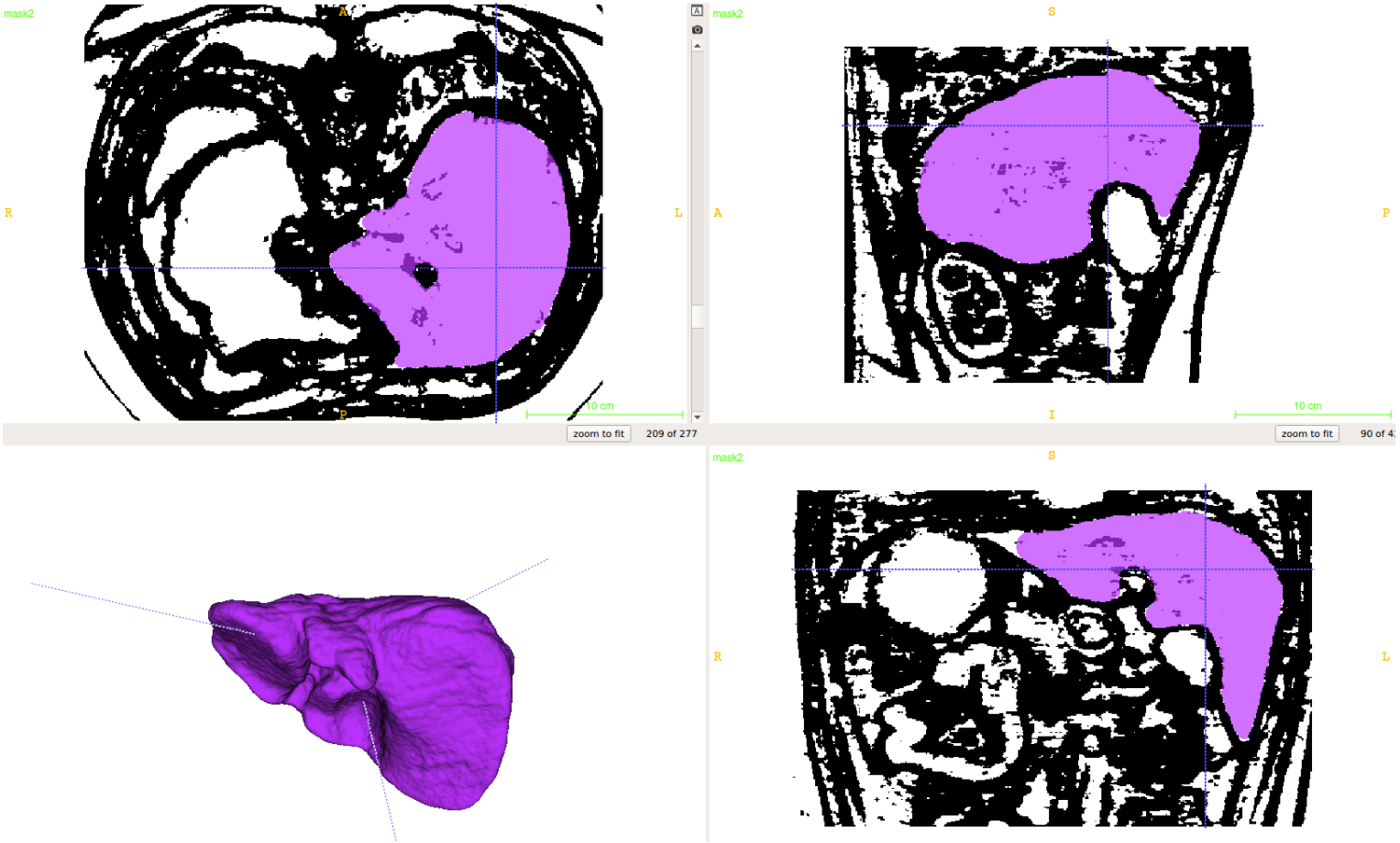

Results

Results of entropy computation on $3 \times 3 \times 3$ vox neighborhood on CPU и GPU.

The GPU version was executed on NVIDIA graphic card GeForce GT 740M, CPU version on Intel Core i7 CPU

Number of voxels	Time, c	
	CPU	GPU
134217728	4274	620
67108864	1662	219
33554432	852	155
16777216	413	77
8388608	198	37
4194304	95	17
2097152	41	7
1048576	16	3

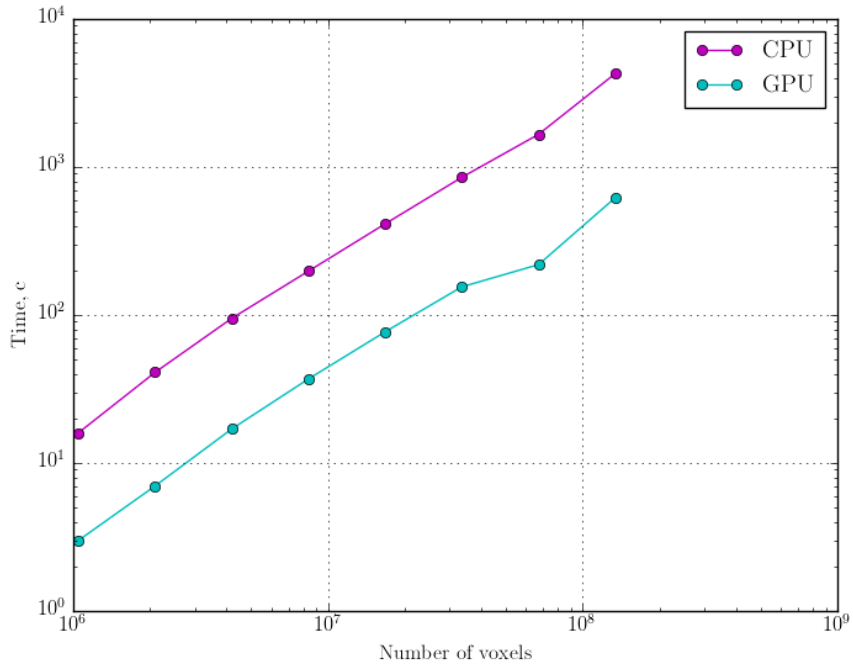

Alexander Danilov, Roman Pryamonosov and Alexandra Yurova. Image segmentation for Cardiovascular Biomedical Applications at different scales. Computation 2016, 4(3),35; doi:10.3390/computation4030035

References

1. Haralick, R.M.; Shanmugam, K.; Dinstein, I. Textural Features for Image Classification. IEEE Transactions on Systems, Man, and Cybernetics 1973, 3, 610–621.
2. R. Achanta, A. Shaji, K. Smith, A.Lucchi, P. Fua, and S. Suesstrunk. SLIC Superpixels Compared to State-of-the-art Superpixel Methods.
3. P.Campadelli, E.Casiraghi, S.Pratissoli, G.Lombardi. Automatic Abdominal Organ Segmentation from CT images. Electronic Letters on Computer Vision and Image Analysis 8(1):1-14, 2009
4. Handels H. Medizinische Bildverarbeitung. Leipzig, 2004.